

# Influence of the anion of Fe<sup>III</sup> salts on the product distribution in the oxidative degradation of a tetrapyridyl ligand

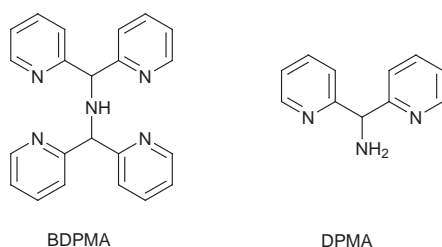
Michael Renz, Catherine Hemmert, Heinz Gornitzka and Bernard Meunier\*

Laboratoire de Chimie de Coordination du CNRS, 205 route de Narbonne, 31077 Toulouse cedex 4, France. Fax: +33 5 61 55 30 03, E-mail: bmeunier@lcc-toulouse.fr

Received (in Montpellier, France) 9th April 1999, Accepted 29th April 1999

We have focused our interest on the tetrapyridyl ligand bis[di(2-pyridyl)methyl]amine (BDPMA) in order to prepare mononuclear non-heme iron(III) complexes as catalyst precursors in oxidation reactions. The investigation of corresponding iron(III) complexes has revealed the fragility of the BDPMA ligand. Different degradation products of the starting ligand have been crystallized and the distribution of these derivatives strongly depends on the nature of the anion in the iron(III) salts.

Aromatic nitrogen heterocycles play an important role in coordination chemistry and many studies have been devoted to transition metal complexes containing such ligands.<sup>1</sup> Due to their electronic, magnetic and redox properties, polynuclear complexes involving two or more metal centers have been extensively studied in supramolecular chemistry and in energy or electron transfer processes.<sup>2</sup> From a bioinorganic chemistry point of view, aromatic nitrogen ligands are of great importance because the *N*-ligand coordination can mimic a part of the environment of the metal active site, particularly in the case of non-heme iron proteins. Many different dinuclear iron complexes have been synthesized in the last past decade, in order to model properties of metalloproteins that bind or activate dioxygen,<sup>3</sup> including hemerythrin,<sup>4</sup> the R2 subunit of ribonucleotide reductase<sup>5</sup> and the hydroxylase component of methane monooxygenase.<sup>6</sup> Several synthetic functional models have also been described, mimicking a class of mononuclear non-heme iron enzymes, catechol dioxygenases,<sup>7</sup> which catalyze the oxidative cleavage of intra- or extra-diol C–C bonds of various catechols using molecular oxygen.<sup>8</sup> These different enzymes are able to oxidize poorly biodegradable man-made molecules.



In our group, we have focused our interest on a tetrapyridyl non-heme iron(III) complex, able to catalyze the oxidative degradation of environmental pollutants<sup>9</sup> such as 2,4,6-trichlorophenol (TCP), a poorly biodegradable molecule.<sup>10</sup> The mononuclear iron(III) complex, Fe(BDPMA)(NO<sub>3</sub>)<sub>3</sub> {BDPMA = bis[di(2-pyridyl)methyl]amine}, is able to catalyze the oxidative degradation of polychlorophenols in the presence of potassium monopersulfate as oxidant.<sup>9</sup> Unfortunately, the oxidation stopped at the quinone level, without formation of ring cleavage products, and the catalyst has a limited lifetime. The fragility of the BDPMA ligand has been evidenced during the preparation of manganese, iron and cobalt complexes.<sup>11</sup> Several degradation products of BDPMA have been identified by X-ray analysis, including fragments

coordinated to metal centers. In the presence of transition metal salts, BDPMA is oxidatively converted in high yield processes to the cationic species 1,3,3-tri(2-pyridyl)-3*H*-imidazo[1,5-*a*]pyridin-4-ium (TPIP, see Scheme 1 for the structure) or to derivatives of di-2-pyridyl ketone (DPK).<sup>11</sup>

In order to fully characterize the BDPMA–iron(III) complexes used in the catalytic oxidations of TCP, we decided to prepare single crystals of the possible complexes generated with BDPMA and different iron(III) salts. Unfortunately, the BDPMA ligand is not stable in the presence of iron(III) salts and we obtained different degradation derivatives depending on the nature of the anion of the ferric salt. Here, we report one of the structures of these degradation products and also the unexpected strong influence of the metal anion in these BDPMA modifications.

## Results and discussion

A yellow complex was obtained in 25–30% yield in one hour at room temperature during attempts to prepare an iron derivative of BDPMA using FeCl<sub>3</sub> as the iron salt. Treatment

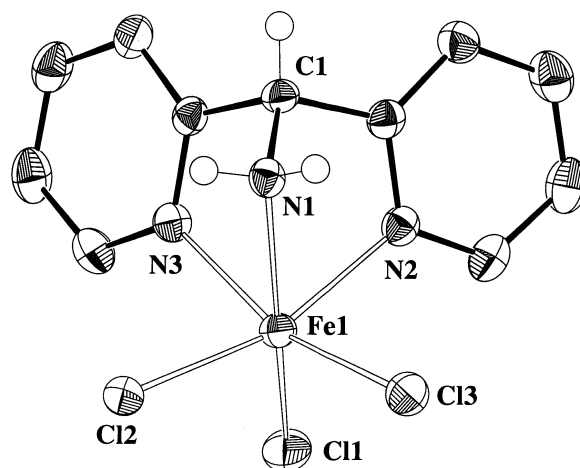


**Fig. 1** Crystal structure of Fe<sup>III</sup>(DPMA)Cl<sub>3</sub> (**3**). Selected bond lengths (Å) and angles (°): Fe1–N1 2.179(2), Fe1–N2 2.186(2), Fe1–N3 2.208(2), Fe1–Cl1 2.261(1), Fe1–Cl2 2.315(1), Fe1–Cl3 2.305(1), N1–Fe1–N2 74.73(8), N1–Fe1–N3 72.75(8), N2–Fe1–N3 80.36(8), N1–Fe1–Cl1 160.70(6), N2–Fe1–Cl1 92.22(6), N3–Fe1–Cl1 91.33(6), N1–Fe1–Cl3 91.28(7), N2–Fe1–Cl3 88.92(6), N3–Fe1–Cl3 162.59(6), N1–Fe1–Cl2 91.58(6), N2–Fe1–Cl2 164.26(6), N3–Fe1–Cl2 88.26(6), Cl1–Fe1–Cl2 98.93(3), Cl1–Fe1–Cl3 102.83(3), Cl3–Fe1–Cl2 99.31(3).

of the crude reaction mixture with KCN in order to demetallate the formed iron complex(es) provided the di-2-pyridyl ketone (58% yield) and traces of DPMA [DPMA = di(2-pyridyl)methylamine], but not the initial ligand BDPMA. These data are reproducible, but we do not understand why the amount of recovered DPMA ligand is below the expected value, a 1 : 1 ratio with the ketone, despite the easy KCN demetallation of the isolated iron(III) complex of DPMA as demonstrated below. It should be noted that BDPMA alone is perfectly stable in solution with or without KCN, but is apparently quickly converted to different products at room temperature in the presence of iron(III) salts.

The KCN demetallation of the yellow complex gave only DPMA, suggesting that this complex contained only DPMA as ligand, which was generated during the decomposition of the initial BDPMA tetrapyridyl ligand in the presence of  $\text{FeCl}_3$ . The X-ray analysis of a single crystal of this yellow complex confirmed that this compound was an iron derivative of DPMA, namely trichloro[di(2-pyridyl)methylamine]iron(III),  $\text{Fe}(\text{DPMA})\text{Cl}_3$ , **3**. The IR spectrum of this monocrystal was identical to that of the yellow powder (see Experimental for data on the main bands). The fragility of BDPMA was already observed when this ligand was mixed with iron(III) nitrate at room temperature, but in this case a different degradation product, namely TPIP (an imidazopyridinium derivative) was obtained.<sup>11</sup>

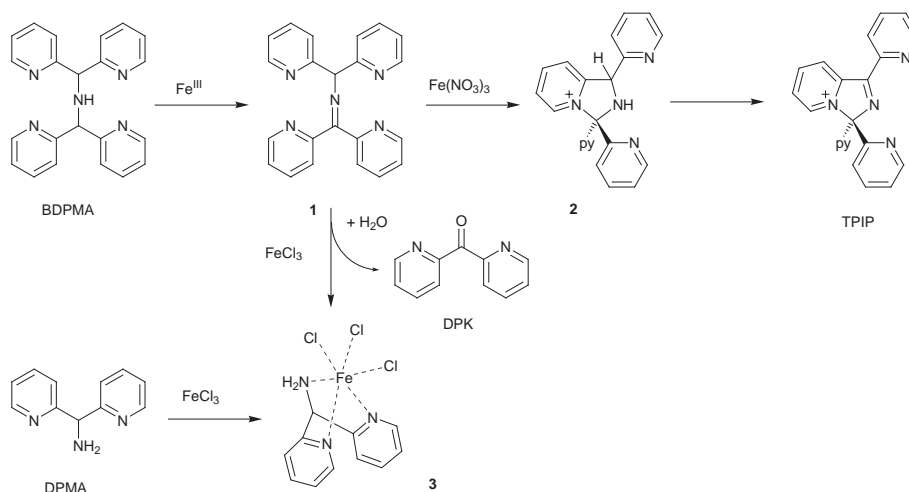
The structure of complex **3** has been determined by X-ray diffraction (Fig. 1). The mononuclear neutral  $\text{Fe}(\text{DPMA})\text{Cl}_3$  entity is best described as a distorted octahedron, in which the two pyridine nitrogens are *cis* coordinated while the secondary amine nitrogen occupies an axial position. The facial coordination mode of the DPMA ligand is similar to that previously reported in the trichloro[bis(pyridin-2-ylmethyl)amine]iron(III) complex ( $\text{FeL}^1\text{Cl}_3$ ),<sup>12</sup> and in contrast to the meridional coordination of the bis(benzimidazol-2-ylmethyl)methylamine ligand observed in the corresponding mononuclear trichloroiron(III) complex ( $\text{FeL}^2\text{Cl}_3$ ).<sup>13</sup> Several features are common to these complexes. Firstly, the  $\text{Fe}-\text{N}_{\text{pyridine}}$  bond lengths are comparable with a mean value of 2.199 and 2.183 Å for  $\text{Fe}(\text{DPMA})\text{Cl}_3$  and  $\text{FeL}^1\text{Cl}_3$ , respectively. Secondly, the three  $\text{Fe}-\text{Cl}$  bond distances are different and the shortest one is always *trans* to the amine nitrogen [ $\text{Fe}-\text{Cl}(2) = 2.261(1)$  Å in  $\text{Fe}(\text{DPMA})\text{Cl}_3$ ]. The major difference in these complexes resides in the  $\text{Fe}-\text{N}_{\text{amine}}$  bond length. The secondary [ $\text{Fe}-\text{N} = 2.216(13)$  Å]<sup>12</sup> and the tertiary [ $\text{Fe}-\text{N} = 2.374(7)$  Å]<sup>13</sup> amine nitrogens in  $\text{FeL}^1\text{Cl}_3$  and  $\text{FeL}^2\text{Cl}_3$ , respectively, are

less strongly bound to the high-spin iron(III) center than the heterocyclic nitrogens. This is also the case in the low-spin iron(II) complex  $[\text{Fe}(\text{DPMA})_2](\text{ClO}_4)_2$ , which exhibits mean bond distances of 1.952(3) Å for  $\text{Fe}-\text{N}_{\text{pyridine}}$  and 1.999(3) Å for  $\text{Fe}-\text{N}_{\text{amine}}$ ,<sup>14</sup> the latter bond lengths being shorter compared to those in iron(III) complexes due to the difference in the spin state of the iron. These observations are in contrast with the surprisingly short  $\text{Fe}-\text{N}_{\text{amine}}$  bond distance of 2.182(2) Å in complex **3**, even though the ligands discussed above are relatively similar in terms of steric constraints and a weaker interaction of the sterically hindered secondary amine would be expected. The noticeable strain in the five-membered chelate rings is illustrated by the following angles: 103.5° for  $\text{Fe}-\text{N}_{\text{amine}}-\text{C}$ , a mean value of 114.4° for  $\text{Fe}-\text{N}_{\text{pyridine}}-\text{C}$ , and 72.7° and 74.6° for  $\text{N}(1)-\text{Fe}-\text{N}(2)$  and  $\text{N}(1)-\text{Fe}-\text{N}(3)$ , respectively.

The surprising structure of this iron(III) complex, containing a fragment of the original BDPMA ligand, could not be explained by the usual oxidative degradation mechanism of BDPMA leading to TPIP (Scheme 1). To obtain additional information on the formation of complex **3**, we decided to synthesize it in a more simple way, directly from the amine DPMA and  $\text{FeCl}_3$ . Indeed, immediately after combining stoichiometric amounts of  $\text{FeCl}_3$  and DPMA in methanol, complex **3** precipitated in high yield. The absence of conductivity showed that complex **3** did not dissociate in solution, confirming its stability.

Since a completely different degradation product of BDPMA, namely TPIP, was observed in the presence of  $\text{Fe}(\text{NO}_3)_3$  (Scheme 1), the complex **4** obtained with DPMA and  $\text{Fe}(\text{NO}_3)_3$  was also synthesized. Because no single crystals could be obtained, complex **4** could not be characterized unambiguously. The FAB mass analysis suggested that, in contrast to complex **3**, two molecules of DPMA are coordinated to the iron center. The conductivity measurement emphasized the different nature of these two iron complexes.  $\text{Fe}(\text{DPMA})_2(\text{NO}_3)_3$  (**4**) behaves as an electrolyte. A conductivity of  $\Lambda_{\text{M}} = 150 \text{ cm}^2 \Omega^{-1} \text{ mol}^{-1}$  was obtained in DMF corresponding to a 2 : 1 electrolyte (literature value for a 2 : 1 electrolyte is in the range of 130–170  $\text{cm}^2 \Omega^{-1} \text{ mol}^{-1}$ ).<sup>15</sup> These two different methods of characterization suggested a hexa- or heptacoordination sphere of iron(III) in complex **4**, involving two tridentate DPMA ligands, one nitrate anion and two nitrates as counterions.

The different coordination spheres around the iron(III) in  $\text{Fe}(\text{DPMA})\text{Cl}_3$  (**3**) and  $\text{Fe}(\text{DPMA})_2(\text{NO}_3)_3$  (**4**) are due to the



**Scheme 1** Oxidative degradation of BDPMA to TPIP initiated by  $\text{Fe}(\text{NO}_3)_3$  or to DPMA initiated and trapped by  $\text{FeCl}_3$ .

stronger coordination ability to the metal center of chlorides when compared to nitrates. The strong influence of the anions  $\text{Cl}^-$  and  $\text{NO}_3^-$  on the different degradation pathways when BDPMA is exposed to iron chloride or iron nitrate is also well illustrated by the different product distributions observed in the oxidative degradation of this tetrapyridyl ligand. In both reaction pathways (Scheme 1), the first reasonable intermediate is the formation of imine **1**, by a two-electron oxidation of BDPMA in the presence of an iron(III) salt. In the presence of  $\text{Fe}(\text{NO}_3)_3$ , the interaction of imine **1** with the iron center should be weaker with respect to  $\text{FeCl}_3$ , due to the greater lability of  $\text{NO}_3^-$  and consequently a weaker stabilization of a possible iron complex. Thus, an imidazolium ring can be formed by intramolecular nucleophilic attack on a pyridine unit, and then continue on to form TPIP. In contrast, with  $\text{FeCl}_3$ , interactions of the pyridine moieties and the iron center should be stronger, probably because of the electronegativity of the  $\text{Cl}^-$  ligands, which helps to remove the electron density provided by the pyridyl ligand to the metal center. Consequently, the intramolecular cyclization is disfavored and the hydrolysis of imine **1** becomes predominant.<sup>16</sup> The amine DPMA, once liberated, will immediately form a stable complex **3** with  $\text{FeCl}_3$ .

## Conclusion

In the present work, we have shown that the BDPMA ligand is oxidatively degraded by  $\text{Fe}^{\text{III}}$  salts. The product distribution in the iron-mediated degradation of this tetrapyridyl ligand is dependent on the nature of the anions in the metallic salts used. As  $\text{Cl}^-$  anions are more electronegative and by far better  $\text{X}^-$  ligands than  $\text{NO}_3^-$  anions, the interaction of  $\text{FeCl}_3$  with the ligand and its degradation products is stronger. The stable interaction of  $\text{FeCl}_3$  with the imine **1** directs the reaction pathway towards the degradation product DPMA, giving rise to complex **3**. Because the intramolecular ring closure by a nucleophilic attack of a pyridine nitrogen is disfavored, the hydrolysis of imine **1** predominates, leading to the formation of the iron complex of the DPMA amine.

## Experimental

Commercially available reagents and all solvents were purchased from standard chemical suppliers and used without further purification. Di(2-pyridyl)methylamine (DPMA) and bis[di(2-pyridyl)methyl]amine (BDPMA) were synthesized according to literature methods.<sup>17</sup> Elemental analyses were carried out by the "Service de Microanalyse du Laboratoire de Chimie de Coordination." Mass spectrometry analyses were performed on a Nermag R1010 apparatus [ $\text{FAB}^+/\text{meta}$ -nitrobenzyl alcohol (MNBA) in DMSO] by the "Service de Spectrométrie de Masse de Chimie UPS-CNRS de Toulouse."  $^1\text{H}$  NMR spectra were run on a Bruker AM 250 (250 MHz), chloroform as internal standard. UV-visible spectra were obtained on a Hewlett-Packard 8452A diode array spectrophotometer, using cuvettes of 1 cm pathlength. EPR spectra were recorded on a Bruker ESP 300 in X-band, with an ER035 M gaussmeter (NMR probe) and an EIP 548 hyperfrequency meter. Powdered samples were loaded in 3 mm cylindrical quartz tubes. Variable-temperature magnetic susceptibilities were determined by the Faraday method in the range 85–285 K, with a  $\text{HgCo}(\text{SCN})_4$  matrix ( $c/g = 16.44 \times 10^{-6}$  emu cgs). The diamagnetism of the ligands was corrected using Pascal's constants. EPR and magnetism data were obtained by the "Service de Mesures Magnétiques du Laboratoire de Chimie de Coordination." Infrared spectra were recorded on a Perkin-Elmer 983 spectrophotometer and samples were run as KBr pellets. Electrochemical experiments were performed at room temperature in an airtight cell connected to a vacuum argon line. Cyclic voltammograms were

obtained with a three-electrode cell comprised of a platinum working electrode (1 mm diameter), a platinum spiral counter electrode (1  $\text{cm}^2$  apparent surface area, 8 cm long and 0.5 cm diameter) and a SCE reference electrode. For electrolysis experiments, a platinum gauze was used. The supporting electrolyte was  $\text{Bu}_4\text{NPF}_6$  and the solvent  $\text{CH}_3\text{CN}$ .

### Trichloro[di(2-pyridyl)methylamine]iron(III), $\text{Fe}(\text{DPMA})\text{Cl}_3$ (**3**)

**From BDPMA and  $\text{FeCl}_3$ .** BDPMA (100 mg, 0.283 mmol) and  $\text{FeCl}_3 \cdot 6\text{H}_2\text{O}$  (70 mg, 0.260 mmol) were dissolved separately in a total volume of 1 mL MeOH. The solutions were combined and stirred at room temperature for 1 h. The solvent was evaporated and the residue dried under vacuum. This reddish brown residue was extracted with dichloromethane and the remaining yellow powder (obtained in 25–30% yield) analyzed as an iron(III) complex. After treatment of this yellow powder with excess KCN, the released ligand was obtained in low yield and identified as being DPMA, not BDPMA. In order to fully characterize this complex, 10 mg of the yellow material were dissolved in a minimum of ethanol. After three weeks, a long (3 mm) orange crystal suitable for X-ray analysis was obtained. This complex was in fact the iron derivative of DPMA, namely trichloro[di(2-pyridyl)methylamine]iron(III),  $\text{Fe}(\text{DPMA})\text{Cl}_3$ , **3**. The IR spectrum of this monocrystalline material was identical to that of the initial yellow powder (main bands at 3289, 3233, 1608, 1600, 1467, 1446, 1296, 1285, 1054, 1024, 858, 832 and  $789\text{ cm}^{-1}$ ).

**Demetallation.** The reaction was first performed as described above. After stirring for 1 h, the solvent was evaporated and the crude reaction mixture dissolved in 10 mL  $\text{CH}_2\text{Cl}_2$ . KCN (600 mg, 9.21 mmol, 32.5 equiv.) dissolved in 10 mL of  $\text{H}_2\text{O}$  was added to the organic solution and the heterogeneous mixture vigorously stirred for 2 h. The organic layer was then washed with  $\text{H}_2\text{O}$  ( $5 \times 50$  mL) and dried with  $\text{MgSO}_4$ . After evaporation of the solvent, 30 mg (58%) of di-2-pyridyl ketone and traces of the DPMA amine were obtained and characterized by  $^1\text{H}$  NMR (250 MHz,  $\text{CDCl}_3$ ). Di-2-pyridyl ketone is commercially available.

**Control reaction.** 50 mg (0.142 mmol) of BDPMA was dissolved in 0.5 mL MeOH and stirred for 1 h. The solvent was evaporated and the residue dissolved in 5 mL  $\text{CH}_2\text{Cl}_2$ . 300 mg (4.61 mmol) of KCN and 35 mg (0.130 mmol) of  $\text{FeCl}_3$  in 5 mL of  $\text{H}_2\text{O}$  were added to the organic solution and the heterogeneous mixture vigorously stirred for 2 h. After the treatment described above, 42 mg (84%) of BDPMA was isolated and characterized by  $^1\text{H}$  NMR (250 MHz,  $\text{CDCl}_3$ ) (see reference 17).

**From DPMA and  $\text{FeCl}_3$ .** DPMA (200 mg, 1.08 mmol) and  $\text{FeCl}_3 \cdot 6\text{H}_2\text{O}$  (270 mg, 1.00 mmol) were dissolved separately in a total volume of 5 mL of MeOH. After combining the two solutions, a yellow solid precipitated immediately. After additional stirring for 30 min, the solid was collected by filtration and dried under vacuum. A yellow microcrystalline powder (316 mg, 91%) was obtained. Anal. calc. for  $\text{FeC}_{11}\text{H}_{11}\text{N}_3\text{Cl}_3$ : C 38.03; H 3.19; N 12.09. Found: C 37.83; H 3.20; N 11.63%. FAB-MS,  $m/z$  (%): 311 (12) [ $\text{Fe}^{\text{III}}(\text{DPMA})\text{Cl}_2$ ] $^+$ , 276 (60) [ $\text{Fe}^{\text{II}}(\text{DPMA})\text{Cl}$ ] $^+$  (the iron(III) complex is reduced in the mass spectrometer during the analysis). UV-Vis (MeOH),  $\lambda_{\text{max}}/\text{nm}$  ( $\epsilon/\text{mol L}^{-1}\text{ cm}^{-1}$ ): 258 (4516), 324 (3095). IR ( $\text{cm}^{-1}$ , KBr): 3289, 3234, 3152, 1600, 1474, 1466, 1446, 1296, 1285, 1054, 1024, 789, 772, 762, 570.

An EPR measurement on a solid sample showed a very broad resonance around  $g = 2.0$  at 100 K, which could not be assigned unambiguously. A Faraday balance measurement on

a powder sample gave an effective magnetic moment per mononuclear complex of  $5.7 \mu_B$ , which is consistent with a high-spin iron(III) complex. Conductivity of a solution in DMF was  $\Lambda_M = 25 \text{ cm}^2 \Omega^{-1} \text{ mol}^{-1}$ , indicating that complex **3** is neutral (for a 1:1 electrolyte  $\Lambda_M = 65\text{--}90 \text{ cm}^2 \Omega^{-1} \text{ mol}^{-1}$ ).<sup>15</sup> A cyclic voltammogram of  $\text{Fe}(\text{DPMA})\text{Cl}_3$  in  $\text{CH}_3\text{CN}$  (0.1 M tetrabutylammonium hexafluorophosphate, scan rate  $100 \text{ mV s}^{-1}$ ) shows a one-electron (confirmed by bulk electrolysis) quasi-reversible (peak-to-peak separation  $\Delta E_p = 112 \text{ mV}$ ) electrochemical reduction at  $-11 \text{ mV vs. SCE}$ . The  $i_{pc}/i_{pa}$  ratio of 0.64 is indicative of poor chemical stability of the reduced iron(II) species.

**Crystal data for 3.**  $\text{C}_{11}\text{H}_{11}\text{Cl}_3\text{FeN}_3$ ,  $M = 347.43$ , monoclinic,  $P2_1/n$ ,  $a = 11.257(2)$ ,  $b = 8.671(1)$ ,  $c = 14.644(2) \text{ \AA}$ ,  $\beta = 107.33(2)^\circ$ ,  $U = 1364.5(3) \text{ \AA}^3$ ,  $Z = 4$ ,  $\rho_c = 1.691 \text{ Mg m}^{-3}$ ,  $F(000) = 700$ ,  $\lambda = 0.71073 \text{ \AA}$ ,  $T = 183(2) \text{ K}$ ,  $\mu(\text{Mo-K}\alpha) = 1.676 \text{ mm}^{-1}$ , crystal size  $0.5 \times 0.4 \times 0.2 \text{ mm}$ ,  $2.76^\circ \leq \theta \leq 24.09^\circ$ , 10040 reflections (2097 independent,  $R_{\text{int}} = 0.0553$ ) were collected at low temperature using an oil-coated shock-cooled crystal<sup>18</sup> on a STOE-IPDS diffractometer. The structure was solved by direct methods (SHELXS-97)<sup>19</sup> and 175 parameters were refined using the least-squares method on  $F^2$ .<sup>20</sup> Largest electron density residue:  $0.337 \text{ e \AA}^{-3}$ ,  $R_1$  [for  $F > 2\sigma(F)$ ] = 0.0298 and  $wR_2 = 0.0830$  (all data) with  $R_1 = \Sigma ||F_o| - |F_c|| / \Sigma |F_o|$  and  $wR_2 = [\Sigma w(F_o^2 - F_c^2)^2 / \Sigma w(F_o^2)^2]^{0.5}$ .

CCDC reference number 440/117. See <http://www.rsc.org/suppdata/nj/1999/773/> for crystallographic files in .cif format.

#### **$\text{Fe}(\text{DPMA})_2(\text{NO}_3)_3$ (**4**)**

DPMA (200 mg, 1.08 mmol) and  $\text{Fe}(\text{NO}_3)_3 \cdot 9\text{H}_2\text{O}$  (270 mg, 1.00 mmol) were dissolved separately in a total volume of 5 mL of MeOH. A few minutes after combining the two solutions, an orange brown solid precipitated. After stirring for 30 min, the solid was collected by filtration and dried under vacuum. An orange brown microcrystalline powder (288 mg, 47%) was obtained. Anal. calc. for  $\text{Fe}(\text{DPMA})_2(\text{NO}_3)_3 \cdot 2\text{H}_2\text{O}$  ( $\text{FeC}_{22}\text{H}_{26}\text{N}_9\text{O}_{11}$ ): C 40.76; H 4.04; N 19.44. Found: C 41.09; H 3.62; N 19.65%. FAB-MS,  $m/z$  (%): 488 (100)  $[\text{Fe}^{\text{II}}(\text{DPMA})_2\text{NO}_3]^+$ , 303 (79)  $[\text{Fe}^{\text{II}}(\text{DPMA})\text{NO}_3]^+$  (the iron(III) complex is reduced in the mass spectrometer during the analysis).

A Faraday balance measurement on a powder sample gave an effective magnetic moment per mononuclear complex of  $2.6 \mu_B$ , which was consistent with a 80:20 mixture of low- and high-spin iron(III) complexes, respectively. An EPR measurement on a solid sample showed a resonance centered at  $g = 4.6$  at 100 K, which is typical for a high-spin iron(III) species. At room temperature, measurements suggested a mixture of high and low spin in the ground state. The conductivity measurement in DMF gave a 2:1 electrolyte with  $\Lambda_M = 150 \text{ cm}^2 \Omega^{-1} \text{ mol}^{-1}$  (literature value for a 2:1 electrolyte is around  $150 \text{ cm}^2 \Omega^{-1} \text{ mol}^{-1}$ ).<sup>15</sup> This is in accordance

with the mass spectrum, where one nitrate was also coordinated to the metal center.

#### **Acknowledgements**

We are grateful to the CNRS for financial support, especially M. R. for a postdoctoral fellowship. The authors thank D. de Montauzon and A. Mari for electrochemical and magnetic data, respectively. B. Donnadiu is acknowledged for assistance with the X-ray measurements. We thank one of the referees for useful comments.

#### **Notes and references**

- (a) P. J. Steel, *Coord. Chem. Rev.*, 1990, **106**, 227. (b) J. Reedijk, in *Comprehensive Coordination Chemistry*, eds. G. Wilkinson, R. D. Gillard and J. A. McCleverty, Pergamon, Oxford, 1987, vol. 2, 73.
- (a) J.-M. Lehn, *Supramolecular Chemistry*, VCH, Weinheim, 1995; (b) E. C. Constable, *Prog. Inorg. Chem.*, 1994, **42**, 67; (c) V. Balzani, A. Juris, M. Venturi, S. Campagna and S. Serroni, *Chem. Rev.*, 1996, **96**, 759.
- B. J. Wallar and J. D. Lipscomb, *Chem. Rev.*, 1996, **96**, 2625.
- R. E. Stenkamp, *Chem. Rev.*, 1994, **94**, 715.
- A. Åbùg, P. Nordlund and H. Eklund, *Nature (London)*, 1993, **361**, 276.
- A. C. Rosenzweig, P. Nordlund, P. M. Takahara, C. A. Frederick and S. J. Lippard, *Chem. Biol.*, 1995, **2**, 409.
- (a) W. O. Koch and H.-J. Krüger, *Angew. Chem., Int. Ed. Engl.*, 1995, **34**, 2671; (b) H. G. Jang, D. D. Cox and L. Que, Jr., *J. Am. Chem. Soc.*, 1991, **113**, 9200; (c) T. Funabiki, T. Yamazaki, A. Fukui, T. Tanaka and S. Yoshida, *Angew. Chem., Int. Ed.*, 1998, **37**, 513.
- L. Que, Jr. and R. Y. N. No, *Chem. Rev.*, 1996, **96**, 2607.
- C. Hemmert, M. Renz and B. Meunier, *J. Mol. Cat. A*, 1998, **137**, 205.
- (a) A. Sorokin, J. L. Séris and B. Meunier, *Science*, 1995, **268**, 1163; (b) A. Sorokin and B. Meunier, *Acc. Chem. Res.*, 1997, **30**, 470.
- (a) M. Renz, C. Hemmert, B. Donnadiu and B. Meunier, *Chem. Commun.*, 1998, 1635. (b) C. Hemmert, M. Renz, H. Gornitzka, S. Soulet and B. Meunier, *Chem. Eur. J.*, 1995, **5**, 1766.
- R. Viswanathan, M. Palaniandavar, T. Balasubramanian and P. T. Muthiah, *J. Chem. Soc., Dalton Trans.*, 1996, 2519.
- H. Adams, N. A. Bailey, J. D. Crane, D. E. Fenton, J.-M. Latour and J. M. Williams, *J. Chem. Soc., Dalton Trans.*, 1990, 1727.
- P. V. Bernhardt, P. Comba, A. Mahu-Rickenbach, S. Stebler, S. Steiner, K. Várnagy and M. Zehnder, *Inorg. Chem.*, 1992, **31**, 4194.
- W. J. Geary, *Coord. Chem. Rev.*, 1971, **7**, 81.
- It was already surprising that the imine **1** cyclized since we observed in the BDPMA synthesis that the equilibrium between the imine and the starting materials (ketone and amine) is mainly on the side of the substrates.<sup>17</sup>
- M. Renz, C. Hemmert and B. Meunier, *Eur. J. Org. Chem.*, 1998, 1271.
- D. Stalke, *Chem. Soc. Rev.*, 1998, **27**, 171.
- G. M. Sheldrick, *Acta Crystallogr. Sect. A*, 1990, **46**, 467.
- G. M. Sheldrick, *SHELXL-97, Program for Crystal Structure Refinement*, University of Göttingen, Germany, 1997.

Paper 9/02907I